Refined USP25/28 inhibitors with improved selectivity towards c-Myc driven squamous lung cancer cells

Adán Pinto-Fernández [1,2*], Claire Heride[3,4], Andrew P Turnbull[4], Dora Pedroso[3,9], Victoria Smith[3], Lisa Mullee[3], Wojciech W Krajewski[4], Cameron Bell[4], Anthony Varca[5], Thomas Charlton[2], Dylan Jones[2], Tom McAllister[6], Roman Fischer[2], Elena Navarro-Guerrero[2], Daniel Ebner[2], Akane Kawamura[6], Sun Kim[7,10], Dave Guerin[7,11], Tim R Hammonds[4,12], Jeffrey Kearns[7,13], Neil Jones[4], Sara J Buhrlage[5], David Komander[8], Sylvie Urbé[3], Michael J Clague[3*], Benedikt M Kessler[1,2*]

[1] Chinese Academy of Medical Sciences Oxford Institute, Nuffield Department of Medicine, Oxford, UK
[2] Target Discovery Institute, Centre for Medicines Discovery, Nuffield Department of Medicine, Oxford, UK
[3] Biochemistry, Cell and Systems Biology, Institute of Systems, Molecular and Integrative Biology, University of Liverpool, Crown St., Liverpool L69 3BX,UK
[4] Cancer Research Horizons, 2 Redman Place, London E20 1JQ, UK
[5] Department of Cancer Biology and the Linde Program in Cancer Chemical Biology, Dana-Farber Cancer Institute, Boston, MA, USA
[6] Chemistry Research Laboratory, University of Oxford, Oxford, UK; Chemistry, School of Natural and Environmental Sciences, Newcastle University, Newcastle Upon Tyne, UK
[7] FORMA Therapeutics, Watertown, Boston, MA, USA
[8] Ubiquitin Signalling Division, The Walter and Eliza Hall Institute of Medical Research, Melbourne, Victoria, AU
[9] Present address: GIMM - Gulbenkian Institute for Molecular Medicine, Edifício Egas Moniz Avenida Professor Egas Moniz, 1649-028 Lisbon, Portugal
[10] Present address: Incyte, Philadelphia, USA
[11] Present address: Molecular Design Consulting LLC, Boston, USA
[12] Present address: University of Leicester, UK
[13] Present address: Novartis Institutes for BioMedical Research (NIBR), Cambridge MA, USA

* Corresponding authors:

Benedikt M Kessler	benedikt.kessler@ndm.ox.ac.uk
Adán Pinto-Fernández	adan.pintofernandez@ndm.ox.ac.uk
Michael Clague	clague@liverpool.ac.uk

Running Title: Refined USP25/28 inhibitors selectively target squamous lung cancer

Abbreviations: c-MYC – oncogene transcription factor, CCND1 – cyclin D1, USP28 – ubiquitin specific protease 28, proteomics, CRISPR, MS/MS – tandem mass spectrometry, DUB inhibitor

Word count: Abstract – 171 words; main text – 3779 words

Authors emails & ORCID numbers

Adán Pinto-Fernández	adan.pintofernandez@ndm.ox.ac.uk	0000-0003-1693-9664
Claire Heride	Claire.heride@cancer.org.uk	0000-0003-1927-9577
Andrew P Turnbull	Andrew.turnbull@cancer.org.uk	
Wojciech W Krajewski	Wojciech.krajewski@cancer.org.uk	
Cameron Bell	Cameron.bell@cancer.org.uk	
Dora Pedroso	dora.pedroso@gimm.pt	0000-0002-5735-5094
Vicky Smith	victoriaesmith@hotmail.co.uk	
Lisa Mullee	lisamullee@gmail.com	
Anthony Varca	Anthony_Varca@dfci.harvard.edu	0000-0002-6308-2491
Thomas Charlton	tom.charlton@cantab.net	0009-0002-4267-1876
Dylan Jones	Dylan_t_jones@yahoo.co.uk	
Tom McAllister	tom.mcallister@ncl.ac.uk	0000-0001-6906-4510
Roman Fischer	roman.fischer@ndm.ox.ac.uk	0000-0002-9715-5951
Elena Navarro-Guerrero	elena.navarroguerrero@ndm.ox.ac.uk	0000-0001-8076-1480
Daniel Ebner	daniel.ebner@ndm.ox.ac.uk	0000-0002-6495-7026
Akane Kawamura	akane.kawamura@ncl.ac.uk	0000-0003-1169-5082
Sun Kim	skim@incyte.com	
Dave Guerin	guerindj@gmail.com	
Tim Hammonds	trhconsulting@outlook.com	
Jeffrey Kearns	jeff.kearns@novartis.com	
Neil Jones	neil.jones@cancer.org.uk	
Sara J Buhrlage	saraj_buhrlage@dfci.harvard.edu	0000-0003-4562-1823
Sylvie Urbé	urbe@liverpool.ac.uk	0000-0003-4735-9814
David Komander	dk@wehi.au.edu	0000-0002-8092-4320
Michael J Clague	clague@liverpool.ac.uk	0000-0003-3355-9479
Benedikt M Kessler	benedikt.kessler@ndm.ox.ac.uk	0000-0002-8160-2446

SUMMARY (171 words)

The ubiquitin specific protease 28 (USP28) is implicated in tumorigenesis by controlling the turnover of the oncogene c-MYC and the ubiquitin ligase FBW7. Here, we describe small molecule inhibitors of USP25 and USP28, leading to cancer cell cycle arrest and death. However, genetic deletion of USP25/28 does not replicate this effect. An integrated –omics approach revealed off-target effects for thienopyridine carboxamide compounds upon the translation apparatus. Chemoproteomics and biochemical analyses suggested binding of the compound to a region near the ribosome complex polypeptide exit tunnel. Structural analysis of a USP28-inhibitor complex enabled the design of modified USP25/28 inhibitor molecules which minimized translation-related off-target effects. In distinction to earlier compounds, the optimized inhibitors were non-toxic to breast cancer cells yet retained potent anti-proliferative activity in squamous lung carcinoma cells, where USP28 is associated with disease progression. Together, our results demonstrate that refined USP25/28 inhibitors can selectively suppress tumor growth by targeting the TP63–FBW7–c-MYC signaling axis, offering a more precise therapeutic strategy for treating squamous lung cancers whilst minimizing undesired cytotoxicity.

INTRODUCTION

Eliminating or inactivating oncogenes and their corresponding protein products remains a strong therapeutic strategy against cancer. KRAS mutant variants driving tumorigenesis have successfully been targeted with selective small molecules [1,2], but this has proven challenging for oncogenes that encode transcription factors, such as c-MYC, ETS, ELK and MLC-1 [3]. Selective induction of their degradation and removal can be achieved by harnessing the ubiquitin system, either through small molecule "degraders", heterobifunctional PROteolysis TArgeting Chimeras (PROTACs), molecular glues or by interfering with the removal of poly-ubiquitin chains from protein substrates by targeting deubiquitylating enzymes (DUBs) [4]. Small molecule inhibitors against DUBs have recently attracted considerable attention, initially for USP7 [5–9], but also for other DUBs including USP25/28 [10–13]. This interest in targeting USP28 was prompted by findings that c-MYC oncogene protein turnover is dependent on the ubiquitin E3 ligase FBW7 [14] and opposed by the ubiquitin specific proteases USP28 and USP36 [15–18]. USP28 deletion and missense mutations have been proposed to affect 53BP1-dependent DNA repair pathways [19,20], p53 stabilisation[21], centrosome loss and associated cell-cycle prolongation in cancer [22–24]. Growth of several tumour types apparently depends on USP28, such as esophageal cancer [25], ovarian clear cell carcinoma (CCC) [26], gastric cancer [27], non-small-cell lung cancer (NSCLC) [28], lung squamous cell carcinoma (SCC) [29] and clear cell renal cell carcinoma (ccRCC) [30], many of which are c-Myc-dependent and p53 deficient. USP28 may also act as a tumour suppressor in melanoma [31], breast and liver carcinogenesis [32], possibly through the p53BP1-p53-p21-USP28 axis including caspase-8 [19,23,33], requiring wildtype p53 and preserving USP28-53BP1 interactions [21]. Other, more tissue-specific factors, such as the squamous epithelial enriched transcription factor Δ-Np63, may be targeted by USP28 specifically in lung squamous cell cancer (LSCC), but not in the adenocarcinoma counterpart LADC [29,34]. Several USP28 small molecule inhibitors have been described, such as AZ1 [12], Vismodegib (VSM) [35], bin-01-07-07 & derivatives [36], FT206 [13], Otilonium bromide [11] and CT1113 [37]. Reduced squamous lung cancer growth *in vivo* was recapitulated with the small molecule inhibitors AZ1 [29], FT206 [13] and CT1113 [38], affecting c-MYC, LSD1 and Δ-Np63 levels. AZ1, VSM and FT206 all cross-react with USP25 due to its close homology with USP28 [39], sharing a common binding mode wedged between the finger and α5 domains [40–42]. This offers an additional opportunity for treatment of pancreatic cancer, for which USP25 has been implicated in progression [43]. However, cellular toxicity outside the c-MYC-LSD1-

Δ-Np63 axis has been observed most with these inhibitors [12,29,35]. Also, no marked small molecule based selectivity towards either USP28 nor USP25 has been achieved, despite emerging molecular insights in the mechanism of USP25/28 inhibition [40,41].

In the present study, we compared the properties of USP25/28 small molecule inhibitors generated from different chemical scaffolds and their effects on cancer cells. The functional discrepancy between USP28 deletion and chemical inhibition, studied most prominently with thienopyridine carboxamide inhibitors, was determined to be due to off-target effects upon protein translation. Structure aided design yielded refined USP25/28 inhibitors with little or no effect on protein translation that retained their potency in selectively affecting growth of squamous lung cancer cells.

RESULTS

Profiling USP28 inhibitors for selectivity and cellular target engagement

The finding that USP28 plays a key role in LSCC tumour maintenance prompted us to identify small molecule inhibitors against this deubiquitylase. A small molecule discovery campaign based on the ubiquitin-rhodamine cleavable assay yielded a panel of compounds sharing a thienopyridine carboxamide chemical scaffold with inhibitory activity. These compounds were selective for USP28 and USP25 [44,45] when tested using the Ubiquitin-propargylamide (Ub-PA) active site probe as a substrate (**Figure 1a**). The identified compounds FT206 [13], FT224 (**Figure 1b**), FT811 (**Figure S1a,b**, left panel) share a thienopyridine carboxamide scaffold similar to B55 and analogues [46]. However, they represent a different chemical class from the previously described benzylic amino ethanol based inhibitor AZ1 (**Figure S1a, b**, right panel) [12], Otilonium bromide [11] or Vismodegib [35,41]. As shown previously for FT206, FT224 is also selective for USP28 and USP25 at a cellular level as measured by an activity-based probe profiling (ABPP) assay, profiling 36 endogenous DUBs in MCF-7 breast cancer cells (**Figure 1d, e**).

USP28 deletion and chemical inhibition alter cell cycle progression and the USP28-FBW7 network

We next explored whether USP25/28 inhibitors had any effects on regulating cell cycle progression. This may occur via altering protein levels of shared USP28/FBW7 substrates, such as c-Myc (and N-Myc) and Cyclin D1 (**Figure 2, S2**). Indeed, USP25/28 chemical inhibition by FT224 or FT811 for 4 and 24 hrs affected levels of Cyclin D1/B1 and to some extent Aurora kinase A (**Figures 2a, S2a, b**), but this was independent of the cellular *FBW7* status. As reported [47,48], *FBW7* deletion elevated c-MYC and Cyclin E1 protein levels (**Figure S3a, b**), but independently of FT224. An overall decrease in S-phase progression was noted upon 24 hour exposure to FT224 (**Figure 2b**), associated with altered protein abundance of Cyclin D1, Cyclin E1 and a decrease of CDK1 phosphorylation (**Figure 2c**). Cyclin D1 mRNA levels were unaffected, suggesting that FT224's mechanism of action is at the posttranscriptional level (**Figure S3c**). These effects were phenocopied by USP28 siRNA knockdown to some extent as demonstrated also by reduced levels of Rb S795 phosphorylation and CDKN1/p21Cip1 and Cyclin D1 protein levels (**Figure 2d**). We observed reduced c-MYC and CCND1 levels in a time- and concentration-

dependent manner, partially rescued by combining USP25/28 inhibition with proteasomal blockade using epoxomicin or interfering with Cullin E3 ligase mediated ubiquitylation with the NEDDylation inhibitor MLN4294 in HCT116 (**Figure S3d**) and MCF7 human breast cancer cells (**Figure S3e**), suggesting ubiquitin mediated alterations in the USP28-cMYC-FBW7 network.

Thienopyridine carboxamide inhibitor affects cell viability independently of USP25/28

To test the correlation between USP28 chemical inhibition and genetic deletion mediated effects on the cell cycle, we knocked out (KO) the *USP28* gene in a range of cell lines of different cancer indications such as breast cancer (MCF-7), chronic myeloid leukaemia (HAP1) and colorectal cancer (HCT116). This resulted in complete or partial reduction of USP28 protein expression (**Figure 2, S4, S5**). Remarkably, cell proliferation of MCF-7 WT and USP28 KO cells were indistinguishable, irrespective of USP25 depletion by siRNA, in contrast to chemical inhibition with FT224 (**Figure 2e-g**). These results indicated the existence of potential off-target effects of this thienopyridine carboxamide-based USP25/28 inhibitor. To confirm and explore this further, USP28 KO HCT116 colorectal cancer cells were generated (**Figure S4a**). Suppression levels of USP28 expression varied between USP28 CRISPR knockout clones (**Figure S4b**), but a correlation could be observed between the protein levels of USP28 and CyclinD1 (**Figure S4c-e**). Analysis of USP28 KO clones 98-3 and 99-2 resulted in partial reduction of Cyclin D1 levels as compared to the WT control clones 99-9 and 98-17, respectively, which was further decreased by adding inhibitors FT224 or FT811 (**Figure S5a, b**), confirming the polypharmacological nature of these inhibitors. Taken together, we noted clear discrepancies between USP25/28 chemical inhibition and deletion on cell viability and substrate abundances along the USP28-FBW7 axis.

Mapping USP25/28 thienopyridine carboxamide inhibitor off-target binding in the ribosome complex

To explore off-targets of these compounds, we generated a biotinylated USP25/28 inhibitor FT224 derivative, FT639, that retained USP28 inhibitory activity *in vitro* and enriched USP25/28 in pulldown experiments (**Figure 3**). Chemoproteomics experiments conducted using different bead types, various stringency of buffer conditions and increased amounts of the biotinylated inhibitor probe revealed significant enrichment of inhibitor probe-reacted USP28 versus untreated (**Figure 3a**, lower right panel). We observed a dose-dependent enrichment of components of the

translation machinery including RPS27L, EEF2 and RRBP1 (**Figures 3b,c** – left, middle and right panels). Most strikingly, RPS27A and RPS27L, enriched with FT639 identified by quantitative MS, were confirmed by immunoblotting (**Figure 3d**). DHX29, IGF2BP3, EEF2 and DSP were also detected consistently across the different experiments/conditions, but not in controls (**Figure 3b**). Some of these interactors are located near the ribosome mRNA channel, reminiscent to the binding region of CHX near the tRNA E-site of the ribosomal 60S subunit [49] (**Figure 3e**). Combined, our data suggests that FT224 does target USP25/28, but also has an off-target near the nascent polypeptide exit tunnel of the ribosome complex (**Figure 3e**).

USP25/28 thienopyridine carboxamide inhibitors affect protein translation

We performed orthogonal assays to probe inhibitor's effects on protein synthesis (translation activity) in cellular and biochemical assays (**Figure 4**). First, a SUnSET assay [50], measuring the synthesis of nascent polypeptide chains by capping with puromycin, revealed a strong inhibitory effect of FT811 in a dose-dependent manner (**Figure 4a**), consistent with USP28 inhibitor's effect on reducing levels of short-lived proteins, not rescuable by subsequent addition of proteasome inhibitor (**Figure 4b**). Second, we conducted the O-propargyl-puromycin (OPP) assay to visualise and quantitate nascent polypeptides in cells using fluorescence microscopy. We compared USP28 inhibitors FT224, FT206 and FT811 to the USP7 inhibitor FT671 [8] as well as cycloheximide and bortezomib (Bz) as positive and negative controls, respectively. Strikingly, sub-micromolar concentrations of USP28 inhibitors affected protein translation in a similar manner to cycloheximide (CHX) (**Figure 4c-e**). Finally, we performed an *in vitro* assay using purified rabbit reticulocyte lysates containing the machinery needed to translate exogenous mRNA only. Translation of Luciferase mRNA was inhibited by FT224 in a dose dependent manner (**Figure S6a,b**). In contrast, FT671, a USP7 inhibitor, and AZ1 (FT214), another USP25/28 inhibitor based on a completely different chemical scaffold [12], did not show any effect in this assay (**Figure S6b**), further suggesting that thienopyridine-based USP25/28 inhibitors bind inside the translation apparatus. This is both scaffold selective and independent of USP28 as HAP-1 wildtype and HAP1 USP28 KO cells revealed no difference in de novo protein synthesis as assayed by puromycin incorporation (**Figure S6c-e**). Consistent with a compound-dependent effect on protein translation, we observed activation of mTOR downstream signalling factors regulating protein translation such as p70S6K and S6RP (**Figure 4f**). Intracellular depletion of ubiquitin has been associated with cellular toxicity and aberrant translation [50]. Consistent with translation interference,

we observed a dose-dependent depletion of ubiquitin by treatment with FT224 (**Figure S6f**). Taken together, we conclude that thienopyridine carboxamide based inhibitors may have an off-target effect that decreases protein translation.

USP28 enzyme-inhibitor structures reveal conserved features for on-target activity

To understand the molecular basis for the poly-pharmacology of these compounds, a crystal of the insert-deleted apo form of the human USP28 catalytic domain was obtained and soaked with the thienopyridine scaffold-based inhibitor, FT592 (**Figure 5, S7a**), a chemical analogue of CRT305/FT224 (**Figure 1b**). The USP28-FT592 complex highlights the molecular basis of compound selectivity. FT592 resides in a cleft formed by α1, α2, α5 and α6 of the thumb subdomain, and β5, β8, β12, β13 and β14 of the palm subdomain (**Figure 5a, 5b**). The USP28-FT592 complex superimposes on apo form insert-deleted USP28 (PDB code 6HEH) with an r.m.s.d. of 1.02 Å (Cα atoms; 314 residues aligned; **Figure S7b**). A rotation of ~3.8° coupled with a translation of ~2 Å (pivoted about residue L273), displaces α5 in the USP28- FT592 complex compared with the apo form structure, expanding the pocket in which FT592 resides (**Figure S7b, c**). The thienopyridine moiety sits in a pocket flanked by S179, L180, H261, L264, F292, Q315, T364, and M646, and directly hydrogen bonds to the side chain amide of Q315 (**Figure 5b**). In addition, the central amide moiety of FT592 hydrogen bonds to the side chain carboxyl of E366. The imidazole substituent is positioned in the channel that usually accommodates the ubiquitin substrate C-terminal tail. Compared with the ubiquitin-propargylamide (UbPA)-bound complex of insert-deleted USP28 (PDB code 6HEI), there is a steric clash between the imidazole substituent and the side chain of L73 of the UbPA substrate, preventing the substrate from binding and being cleaved (**Figure 5c, 5d**). The binding mode of FT592 is analogous to previously reported inhibitors including FT206, AZ1, and Vismodegib, which wedge between α5 and the palm subdomain preventing transition to a substrate-binding competent state [11,40,42] (**Figure S7d, e, f-g**).

A hallmark unique to USP25 and USP28 is that they both form homodimers, with USP25 additionally forming homotetramers via an autoinhibitory element from a neighbouring molecule [39,51,52]. The USP28-FT592 complex, and the catalytic domain of USP25 (PDB code 6HEL) superimpose with an r.m.s.d. of 1.27 Å (Cα atoms; 299 residues aligned; **Figure 5e**). This places FT592 in the autoinhibitory motif (AIM) binding pocket of the catalytic domain of USP25, which is responsible for autoinhibition by tetramerization of USP25. There are 21 residues residing within

5 Å of FT592 in the USP28-FT592 complex (V176, S179, L180, V256, S257, T260, H261, L264, F292, G314, Q315, T364, E366, F370, L590, H592, A596, Y601, Y643, C644, and M646). These residues are fully conserved in human USP25, explaining why FT592 also inhibits USP25 catalytic activity. The 14-mer AIM is highly conserved in USP25 amongst mammalian species and centres on a Pro-Phe motif (P521-F522), whereas the equivalent sequence in USP28 lacks conservation [39]. Superposition of USP28-FT592 on the autoinhibited USP25 tetramer reveals that the Pro-Phe motif of the adjacent dimer overlays with the position of the thienopyridine moiety in the USP28-FT592 complex (**Figure 5e**). In contrast, the USP7 inhibitors, GNE6640 (PDB code 5UQV) and GNE6776 (PDB code 5UQX), are largely solvent exposed and lie between α5 and α6 at the interface between the palm, fingers, and thumb subdomains in the catalytic domain of USP7, in a pocket that partially overlaps with the FT592 pocket in USP28 (**Figure S7h-i**). The phenol substituent of GNE6640 and GNE6776 overlays with P521 of the Pro-Phe motif in USP25. The region corresponding to the AIM pocket in USP25/28 appears larger in size as compared with USP7 (**Figure 5f**) and USP8 (**Figure 5g**), as the residues surrounding it have in many cases sterically less demanding side chains (e.g., T364 in USP25/USP28 vs. H403 in USP7 or C644 in USP25/USP28 vs. M515 in USP7 and in many other DUBs), which explains the unique selectivity of these inhibitors for USP25 and USP28.

Optimising different USP25/28 inhibitor chemical scaffolds to remove off-target effect on translation

Structural information allowed the exploration of a systematic structure activity relationship (SAR) to preserve critical elements for selective USP25/28 inhibition and vary other parts of small molecules that may underlay the observed effects in protein translation. To this end, a panel of different molecule derivatives encompassing various chemical scaffolds including thienopyridine carboxamides, but also a variety of different chemical moieties, were generated and tested for USP28 enzyme inhibition (**Figure S8-10**), demonstrating potency and USP25/28 selectivity in an ABPP assay [36,53,54]. To test their potential off-target activity on protein translation, an OPP assay was used in MCF-7 cells as described above. We found that a subset of compounds with structural differences to the FT compounds, showed much reduced or no inhibition of protein synthesis as compared to FT811 (**Figure 6a-c**), correlating with structural features that preserved USP25/28 inhibition capacity (**Figure S11**). Interestingly, and confirming our previous

observations, cell viability measurements of MCF-7 breast cancer cells correlated with the compound's potency to inhibit protein translation (**Figure 6d, S8**).

Improved selectivity towards squamous lung cancer cell susceptibility due to on-target USP28 inhibition

USP28 dependence is linked to cancer types driven by c-Myc and p63, such as squamous lung cancer [13,29,55]. To test this, we exposed wildtype and USP28 KO MCF-7 breast cancer cells as well as H-520 squamous lung cancer cells to refined USP25/28 inhibitors with reduced or lack of potency in protein translation inhibition, namely bin-07-07 and AV-24-34 (**Figure 7**). As positive controls, we used FT224 and bin-01-74, two inhibitors with similar structures and translation inhibition profiles. FT224 and bin-01-74 were, as expected, the most potent cell viability inhibitors in all three cell lines. In contrast, bin-07-07 and AV-24-34, relatively ineffective when exposed to MCF-7 (WT or USP28 KO) breast cancer cells (**Figure 7a, b**), showed a selective inhibition of the viability of H-520 squamous lung cancer cells (**Figure 7c**).

DISCUSSION

Lung squamous cell carcinoma (LSCC) development is characterised by i) mutational loss of p53 and RB1 tumour suppressors, ii) lineage-specific transcription factors, also referred to as lineage oncogenes ASCL1, NEUROD1, POU2F3, inducing a neuro-endocrine (NE) expression programme, iii) inhibition of NOTCH signalling [56] and iv) overexpression of members of the myc family, such as c-MYC, MYCL or MYCN [57]. USP28 small molecule inhibition/deletion affects NOTCH-1, c-MYC, LSD1 and delta-Np63 levels [29,58], but tissue-specific components must also contribute to malignant transformation due to different oncogenic pathways [34]. Targeting USP28 with small molecule inhibitors may reflect an attractive therapeutic strategy against LSCC and potentially other c-MYC-dependent p53 deficient cancer types.

Multiple chemical scaffolds have led to the discovery of USP25/28 inhibitors. This includes thienopyridine carboxamides [44], benzyl ethanolamines [12] and hybrid scaffolds [54], with inhibition potencies between high nM to the mid μM range. CT1113 [59,60], which shows a clear similarity to the previous reported FT206 [13], is considered in clinical trials against myeloid leukemia, hemic and lymphatic diseases [37,61]. For thienopyridine carboxamides, we observed cell viability effects irrespective of the presence or absence of USP28, thereby suggesting off-target effects. This is also seen with other USP25/28 inhibitors, such as Otilonium bromide, an approved drug for treating irritable bowel syndrome [11] and Vismodegib, previously described as a hedgehog signalling inhibitor [35,62], both of which were originally designed for other clinical targets. Thienopyridine carboxamide scaffold containing medicinal drugs have been previously described, for example for inhibiting HIV Rev-response elements (PRE) protein complexes [63]. No noticeable off-target effects in translation/protein synthesis have been reported for these, suggesting that further derivatisation of thienopyridine carboxamide moieties to optimise targeting USP25/28 may have inadvertently increased affinity to off-target(s) in the translation apparatus.

Uncovering off-targets is challenging. Several approaches were used including chemoproteomics (**Figure 3**), genetic and proteomics screens and cellular adaptation experiments (see Supplementary Information for additional details and an extended discussion). These extended analyses confirmed target-independent effects, all pointing towards an alternative mechanism of action for thienopyridine carboxamides within the translation machinery.

Another hallmark was the observed decrease in global levels of conjugated ubiquitin upon FT224 treatment (**Figure S6f**), somewhat reminiscent to cycloheximide mediated depletion of ubiquitin

observed in yeast, due to preventing *de-novo* protein synthesis [50]. The potential structural overlap between binding modes within USP25/28 and the tRNA E-site of the ribosomal 60S subunit is not obvious. However, cycloheximide and other compounds, such as lactimidomycin, phyllanthoside, T-2 toxin, deoxynivalenol, verrucarin A, narciclasine, lycorine, nagilactone C, anisomycin, homoharringtonine and cryptopleurine all bind to the same region in the 60S. This may represent the presence of a small molecule "hot spot" [64] that might exert affinity for some thienopyridine carboxamides including FT224.

The USP28 – inhibitor structures provide an opportunity to generate refined inhibitors with minimal off-target effects, by identifying other chemical scaffolds away from the thienopyridine carboxamide moiety, some of which correlated with inhibition of translation (OPP activity) (**Figure S11**). The chemical rationale for removing effects on translation awaits more structural insights into the exact binding mode to the 60S ribosome "hot spot" region. In absence of precise structural insights, an approach was taken to determine the essential structural features for inhibitors to retain selectivity for USP25/28 inhibition. Of note is a possible correlation between how much the USP25/28 inhibitors reach out into the Ub-C-terminal binding channel of USP28 towards the active site and the magnitude of translation inhibition. This observation may provide useful information regarding which parts of the inhibitor molecule need to be preserved to retain USP25/28 inhibition while dialling out off-target effects on translation. Refined USP25/28 inhibitors with minimal or no off-target on translation turned out to be more selective for squamous lung carcinoma in cell-based viability experiments (**Figure 7**). This is consistent with AZ1/FT214 not having any noticeable effect on translation but displaying a clear reduction in the growth of squamous lung carcinoma *in vivo* [29]. *In vivo* potency of small molecule inhibitors may benefit from drug multi-specificity [65], which may be the case for the USP25/28 inhibitor CT1113 [61] as it shares the thienopyridine carboxamide scaffold with the compounds described in this study. Protein translation inhibitors are in various states of clinical evaluation [66].

In summary, the discovery of an off-target effect on protein translation related to the thienopyridine carboxamide moiety reveals insights into multidrug specificity. The development of refined USP25/28 inhibitor scaffolds provides the framework for more potent therapeutics targeting USP28 for the treatment of squamous lung cancer in particular, and perhaps other c-MYC-dependent cancer types in general.

MATERIALS AND METHODS

A detailed description of the materials and methods used in this study can be found in the **Supplementary Information** section of the online article (URL Address).

ACKNOWLEDGEMENTS

We are grateful for critical inputs from members of the Pinto-Fernandez, Kessler and Urbé & Clague laboratories and of the DUB Alliance (Forma Therapeutics). We also thank the Discovery Proteomics Facility, led by Dr Iolanda Vendrell, and Dr Simon Davis and Marie-Laëtitia Thézénas for expert help with proteomics and mass spectrometry analysis. We thank Dr Sebastian Nijman (The Netherlands) for the kind gift of the HAP1 USP28 knockout (KO) cell line. In addition, we thank Dr Ross Chapman (Oxford, UK) for generously providing the MCF7 USP28 knockout (KO) cell line. We also thank Dr Feng Zhang for providing the Human CRISPR Activation Library (SAM v1). This study was funded by Forma Therapeutics. Work in the Kessler laboratory was supported by a John Fell Fund 133/075, the Wellcome Trust (097813/Z/11/Z), the Engineering and Physical Sciences Research Council (EP/N034295/1) and the Chinese Academy of Medical Sciences (CAMS) Innovation Fund for Medical Science (CIFMS), China (grant number: 2024-I2M-2-001-1.

AUTHORSHIP CONTRIBUTIONS

B.M.K., S.U. and M.J.C. conceptualised the study. S.K., D.G., T.H., J.K., N.J., S.J.B., S.U., D.K., M.J.C. and B.M.K. directed projects involved in this study. A.P.F. and C.H. performed and directed biochemical and cell biological experiments. A.P.T. and W.W.K. performed structural studies. C.B., D.P., V.S. and L.M. assisted with the cell biology experiments. A.V., D.G. and S.J.B. designed and synthesised small molecule inhibitors. T.C., T. M.A., A.K. and A.P.F. performed chemical biology experiments. D.J., E.N.G. and D.E. performed genetic screening experiments. A.P.F., C.H., R.F., S.U. and B.M.K. performed data analysis. S.K., T.H., J.K., N.J. and D.K. have contributed to funding via the DUB Alliance supported by Forma Therapeutics. A.P.F., C.H, S.U., M.J.C. and B.M.K. wrote the manuscript. All co-authors have approved the finalised version.

DATA AVAILABILITY

The crystal structure of human USP28 catalytic domain in complex with FT592 was deposited (D_1292155111) and is assigned to the accession code(s) PDB ID 29GK, Extended PDB ID pdb_000029GK.

Mass spectrometry (MS) data are available via ProteomeXchange with identifier PXD075950.

CRISPR sequencing data will be available to download from GEO-NCBI-NIH.

DECLARATION OF CONFLICTS OF INTERESTS

C.H., A.P.T., W.W.K., C.B., N.J. are employees of CRUK Cancer Research Horizon. T.R.H. is employed by TRH Consulting. S.K., D.G., J.K. were employees of FORMA Therapeutics. This work was performed by the DUB Alliance and funded by FORMA Therapeutics.

REFERENCES

1. Wu, X. *et al.* Small molecular inhibitors for KRAS-mutant cancers. *Front. Immunol.* **14**, (2023).
2. Popow, J. *et al.* Targeting cancer with small-molecule pan-KRAS degraders. *Science (1979).* **385**, 1338–1347 (2024).
3. Lewin, B. Oncogenic conversion by regulatory changes in transcription factors. *Cell* Preprint at https://doi.org/10.1016/0092-8674(91)90640-K (1991).
4. Harrigan, J. A., Jacq, X., Martin, N. M. & Jackson, S. P. Deubiquitylating enzymes and drug discovery: Emerging opportunities. *Nature Reviews Drug Discovery* Preprint at https://doi.org/10.1038/nrd.2017.152 (2018).
5. Altun, M. *et al.* Activity-based chemical proteomics accelerates inhibitor development for deubiquitylating enzymes. *Chem. Biol.* **18**, (2011).
6. Reverdy, C. *et al.* Discovery of specific inhibitors of human USP7/HAUSP deubiquitinating enzyme. *Chem. Biol.* **19**, 467–477 (2012).
7. Kategaya, L. *et al.* USP7 small-molecule inhibitors interfere with ubiquitin binding. *Nature* https://doi.org/10.1038/nature24006 (2017) doi:10.1038/nature24006.
8. Turnbull, A. P. *et al.* Molecular basis of USP7 inhibition by selective small-molecule inhibitors. *Nature* **550**, (2017).
9. Lamberto, I. *et al.* Structure-Guided Development of a Potent and Selective Non-covalent Active-Site Inhibitor of USP7. *Cell Chem. Biol.* **24**, 1490-1500.e11 (2017).
10. Liu, Z. *et al.* Discovery of [1,2,3]triazolo[4,5-d]pyrimidine derivatives as highly potent, selective, and cellularly active USP28 inhibitors. *Acta Pharm. Sin. B* https://doi.org/10.1016/j.apsb.2019.12.008 (2019) doi:10.1016/j.apsb.2019.12.008.
11. Xu, Z. *et al.* Otilonium Bromide acts as a selective USP28 inhibitor and exhibits cytotoxic activity against multiple human cancer cell lines. *Biochem. Pharmacol.* **215**, 115746 (2023).
12. Wrigley, J. D. *et al.* Identification and Characterization of Dual Inhibitors of the USP25/28 Deubiquitinating Enzyme Subfamily. *ACS Chem. Biol.* **12**, 3113–3125 (2017).
13. Josue Ruiz, E. *et al.* Usp28 deletion and small-molecule inhibition destabilizes c-myc and elicits regression of squamous cell lung carcinoma. *Elife* **10**, (2021).
14. Davis, R. J., Welcker, M. & Clurman, B. E. Tumor suppression by the Fbw7Ubiquitin

ligase: Mechanisms and opportunities. *Cancer Cell* Preprint at https://doi.org/10.1016/j.ccell.2014.09.013 (2014).

15. Popov, N. *et al.* The ubiquitin-specific protease USP28 is required for MYC stability. *Nat. Cell Biol.* https://doi.org/10.1038/ncb1601 (2007) doi:10.1038/ncb1601.
16. Popov, N., Herold, S., Llamazares, M., Schülein, C. & Eilers, M. Fbw7 and Usp28 regulate Myc protein stability in response to DNA damage. *Cell Cycle* https://doi.org/10.4161/cc.6.19.4804 (2007) doi:10.4161/cc.6.19.4804.
17. Wang, X. *et al.* Targeting deubiquitinase USP28 for cancer therapy. *Cell Death and Disease* Preprint at https://doi.org/10.1038/s41419-017-0208-z (2018).
18. Sun, X. X. *et al.* The nucleolar ubiquitin-specific protease USP36 deubiquitinates and stabilizes c-Myc. *Proc. Natl. Acad. Sci. U. S. A.* https://doi.org/10.1073/pnas.1411713112 (2015) doi:10.1073/pnas.1411713112.
19. Cuella-Martin, R. *et al.* 53BP1 Integrates DNA Repair and p53-Dependent Cell Fate Decisions via Distinct Mechanisms. *Mol. Cell* https://doi.org/10.1016/j.molcel.2016.08.002 (2016) doi:10.1016/j.molcel.2016.08.002.
20. Fong, C. S. *et al.* 53BP1 and USP28 mediate p53- dependent cell cycle arrest in response to centrosome loss and prolonged mitosis. *Elife* https://doi.org/10.7554/eLife.16270 (2016) doi:10.7554/eLife.16270.
21. Belal, H., Ng, E. F. Y., Ohta, M. & Meitinger, F. Cancer-associated USP28 missense mutations disrupt 53BP1 interaction and p53 stabilization. *Nat. Commun.* **16**, 10310 (2025).
22. Knobel, P. A. *et al.* USP28 Is Recruited to Sites of DNA Damage by the Tandem BRCT Domains of 53BP1 but Plays a Minor Role in Double-Strand Break Metabolism. *Mol. Cell. Biol.* https://doi.org/10.1128/mcb.00197-14 (2014) doi:10.1128/mcb.00197-14.
23. Lambrus, B. G. *et al.* A USP28-53BP1-p53-p21 signaling axis arrests growth after centrosome loss or prolonged mitosis. *Journal of Cell Biology* https://doi.org/10.1083/jcb.201604054 (2016) doi:10.1083/jcb.201604054.
24. Meitinger, F. *et al.* 53BP1 and USP28 mediate p53 activation and G1 arrest after centrosome loss or extended mitotic duration. *Journal of Cell Biology* https://doi.org/10.1083/jcb.201604081 (2016) doi:10.1083/jcb.201604081.
25. Weili, Z., Zhikun, L., Jianmin, W. & Qingbao, T. Knockdown of USP28 enhances the radiosensitivity of esophageal cancer cells via the c-Myc/hypoxia-inducible factor-1 alpha pathway. *J Cell Biochem* **120**, 201–212 (2019).

26. Ito, F., Yoshimoto, C., Yamada, Y., Sudo, T. & Kobayashi, H. The HNF-1β-USP28-Claspin pathway upregulates DNA damage-induced Chk1 activation in ovarian clear cell carcinoma. *Oncotarget* https://doi.org/10.18632/oncotarget.24776 (2018) doi:10.18632/oncotarget.24776.
27. Zhao, L. J. *et al.* USP28 contributes to the proliferation and metastasis of gastric cancer. *J. Cell. Biochem.* https://doi.org/10.1002/jcb.28040 (2019) doi:10.1002/jcb.28040.
28. Li, P., Huang, Z., Wang, J., Chen, W. & Huang, J. Ubiquitin-specific peptidase 28 enhances STAT3 signaling and promotes cell growth in non-small-cell lung cancer. *Onco. Targets. Ther.* https://doi.org/10.2147/OTT.S194917 (2019) doi:10.2147/OTT.S194917.
29. Prieto-Garcia, C. *et al.* Maintaining protein stability of ΔNp63 via USP28 is required by squamous cancer cells. *EMBO Mol. Med.* **e11101**, (2020).
30. Ren, Y. *et al.* Targeting USP28 inhibits clear cell renal cell carcinoma growth. *Cell. Signal.* **139**, 112344 (2026).
31. Saei, A. *et al.* Loss of USP28-mediated BRAF degradation drives resistance to RAF cancer therapies. *Journal of Experimental Medicine* https://doi.org/10.1084/jem.20171960 (2018) doi:10.1084/jem.20171960.
32. Richter, K. *et al.* USP28 deficiency promotes breast and liver carcinogenesis as well as tumor angiogenesis in a HIF-independent manner. *Molecular Cancer Research* https://doi.org/10.1158/1541-7786.MCR-17-0452 (2018) doi:10.1158/1541-7786.MCR-17-0452.
33. Müller, I. *et al.* Cancer Cells Employ Nuclear Caspase-8 to Overcome the p53-Dependent G2/M Checkpoint through Cleavage of USP28. *Mol. Cell* https://doi.org/10.1016/j.molcel.2019.12.023 (2020) doi:10.1016/j.molcel.2019.12.023.
34. Prieto-Garcia, C., Tomašković, I., Shah, V. J., Dikic, I. & Diefenbacher, M. USP28: Oncogene or Tumor Suppressor? A Unifying Paradigm for Squamous Cell Carcinoma. *Cells* **10**, (2021).
35. Wang, H. *et al.* USP28 and USP25 are downregulated by Vismodegib in vitro and in colorectal cancer cell lines. *FEBS J.* **288**, 1325–1342 (2021).
36. Varca, A. C. *et al.* Identification and validation of selective deubiquitinase inhibitors. *Cell Chem. Biol.* **28**, 1758-1771.e13 (2021).
37. Xu, J. *et al.* Preclinical testing of <scp>CT1113</scp> , a novel <scp>USP28</scp> inhibitor, for the treatment of T-cell acute lymphoblastic leukaemia. *Br. J. Haematol.* **204**, 2301–2318 (2024).

38. Cai, C. *et al.* The deubiquitinase USP28 promotes esophageal squamous cell carcinoma proliferation by stabilizing ΔNp63 protein. *Cell. Signal.* **143**, 112489 (2026).
39. Gersch, M. *et al.* Distinct USP25 and USP28 Oligomerization States Regulate Deubiquitinating Activity. *Mol. Cell* https://doi.org/10.1016/j.molcel.2019.02.030 (2019) doi:10.1016/j.molcel.2019.02.030.
40. Patzke, J. V. *et al.* Structural basis for the bi-specificity of USP25 and USP28 inhibitors. *EMBO Rep.* **25**, 2950–2973 (2024).
41. Zhou, D. *et al.* Structure-based discovery of potent USP28 inhibitors derived from Vismodegib. *Eur. J. Med. Chem.* **254**, 115369 (2023).
42. Wang, F. *et al. Molecular Basis of USP28 Allosteric Inhibition by Small-Molecule Inhibitor AZ1*. https://papers.ssrn.com/sol3/papers.cfm?abstract_id=4676302 (2024).
43. Nelson, J. K. *et al.* USP25 promotes pathological HIF-1-driven metabolic reprogramming and is a potential therapeutic target in pancreatic cancer. *Nat. Commun.* **13**, 2070 (2022).
44. Zablocki, M.-M. *et al.* CARBOXAMIDES AS UBIQUITIN-SPECIFIC PROTEASE INHIBITORS. Preprint at https://patentscope.wipo.int/search/en/detail.jsf?docId=WO2019032863 (2019).
45. Guerin, D. *et al.* THIENOPYRIDINE CARBOXAMIDES AS UBIQUITIN-SPECIFIC PROTEASE INHIBITORS. 1–361 Preprint at https://patentscope.wipo.int/search/en/detail.jsf?docId=WO2017139778 (2017).
46. Bratt, A. S. *et al.* Pharmacologic interrogation of USP28 cellular function in p53 signaling. *Cell Chem. Biol.* **32**, 1166-1182.e27 (2025).
47. Sancho, R. *et al.* F-box and WD Repeat Domain-Containing 7 Regulates Intestinal Cell Lineage Commitment and Is a Haploinsufficient Tumor Suppressor. *Gastroenterology* **139**, 929–941 (2010).
48. Schülein-Völk, C. *et al.* Dual Regulation of Fbw7 Function and Oncogenic Transformation by Usp28. *Cell Rep.* **9**, 1099–1109 (2014).
49. Garreau de Loubresse, N. *et al.* Structural basis for the inhibition of the eukaryotic ribosome. *Nature* **513**, 517–522 (2014).
50. John, H., S., L. D. & Daniel, F. Ubiquitin Depletion as a Key Mediator of Toxicity by Translational Inhibitors. *Mol. Cell. Biol.* **23**, 9251–9261 (2003).
51. Liu, B., Sureda-Gómez, M., Zhen, Y., Amador, V. & Reverter, D. A quaternary tetramer assembly inhibits the deubiquitinating activity of USP25. *Nat. Commun.* https://doi.org/10.1038/s41467-018-07510-5 (2018) doi:10.1038/s41467-018-07510-5.

52. Sauer, F. *et al.* Differential Oligomerization of the Deubiquitinases USP25 and USP28 Regulates Their Activities. *Mol. Cell* https://doi.org/10.1016/j.molcel.2019.02.029 (2019) doi:10.1016/j.molcel.2019.02.029.
53. Varca, A. C., Casalena, D., Auld, D. & Buhrlage, S. J. Identification of deubiquitinase inhibitors via high-throughput screening using a fluorogenic ubiquitin-rhodamine assay. *STAR Protoc.* **2**, 100896 (2021).
54. Chan, W. C. *et al.* Accelerating inhibitor discovery for deubiquitinating enzymes. *Nat. Commun.* **14**, 686 (2023).
55. Prieto-Garcia, C. *et al.* USP28 enables oncogenic transformation of respiratory cells, and its inhibition potentiates molecular therapy targeting mutant EGFR, BRAF and PI3K. *Mol. Oncol.* **16**, 3082–3106 (2022).
56. Shih, I. M. & Wang, T. L. Notch signaling, γ-secretase inhibitors, and cancer therapy. *Cancer Research* Preprint at https://doi.org/10.1158/0008-5472.CAN-06-3958 (2007).
57. Gazdar, A. F. & Minna, J. D. Small cell lung cancers made from scratch. *Journal of Experimental Medicine* https://doi.org/10.1084/jem.20182216 (2019) doi:10.1084/jem.20182216.
58. Wu, Y. *et al.* The Deubiquitinase USP28 Stabilizes LSD1 and Confers Stem-Cell-like Traits to Breast Cancer Cells. *Cell Rep.* https://doi.org/10.1016/j.celrep.2013.08.030 (2013) doi:10.1016/j.celrep.2013.08.030.
59. Peng, J. *et al.* Identification of a class of potent USP25/28 inhibitors with broad-spectrum anti-cancer activity. *Signal Transduct. Target. Ther.* **7**, 393 (2022).
60. Li, J. *et al.* The deubiquitinase USP28 maintains the expression of the transcription factor MYCN and is essential in neuroblastoma cells. *Journal of Biological Chemistry* **299**, 104856 (2023).
61. Zhou, S. *et al.* Abstract LB367: CT1113, a dual USP25/28 inhibitor, promotes antitumor immunity by preventing YTHDF2-mediated complement activation and potentiates anti-PD-1 therapy. *Cancer Res.* **85**, LB367–LB367 (2025).
62. Aditya, S. & Rattan, A. Vismodegib: A smoothened inhibitor for the treatment of advanced basal cell carcinoma. *Indian Dermatol. Online J.* **4**, 365–8 (2013).
63. Nakamura, R. *et al.* Identification and Optimization of Thienopyridine Carboxamides as Inhibitors of HIV Regulatory Complexes. *Antimicrob. Agents Chemother.* **61**, e02366-16 (2021).
64. Lin, A. *et al.* Off-target toxicity is a common mechanism of action of cancer drugs

undergoing clinical trials. *Sci. Transl. Med.* https://doi.org/10.1126/scitranslmed.aaw8412 (2019) doi:10.1126/scitranslmed.aaw8412.

65. Deshaies, R. J. Multispecific drugs herald a new era of biopharmaceutical innovation. *Nature* **580**, 329–338 (2020).

66. Jia, X. *et al.* Protein translation: biological processes and therapeutic strategies for human diseases. *Signal Transduct. Target. Ther.* **9**, 44 (2024).

FIGURE LEGENDS

Figure 1: USP25/28 inhibitor FT224 cellular target engagement

a Scheme of activity-based protein profiling (ABPP) assay.

b FT224 structure and chemical compound inhibitor properties.

c FT224 potency towards USP28 and USP25 assessed by the ABPP assay in MCF7 cell extracts.

d ABPP-MS assay controls analysed by SDS-PAGE and immunoblotting.

e ABPP-MS of the FT224 cellular DUB target engagement profile in MCF7 cell extracts.

Figure 2: FT224 affects cell cycle progression independent of USP25/28

a HCT116 proteomics-based quantitation of USP28 substrates in FBW7 wildtype (+/+) and knockout (-/-) cells treated with 5μM FT224 or DMSO (control) for 4 hrs.

b FT224 affects MCF7 cells entering into S-phase after 24 hrs.

c FT224 effects on cell cycle regulators after 4 and 24 hrs.

d FT224 or USP28 KD effects on cell cycle regulators after 4 and 24 hrs.

e MCF7 cell viability upon USP28 and/or USP25 knockdown (upper panel), and HAP1 cell viability upon USP28 knockdown (lower panel).

f USP25/28 knockdown efficiencies in MCF7 cells and effects of inhibitor exposure for 24 hrs.

g USP25/28 knockdown efficiencies in HAP1 cells and effects of inhibitor exposure for 3 or 24 hrs.

Figure 3: FT639 Chemoproteomics reveals the USP25/28 inhibitor interactome

a Chemoproteomics strategy for target discovery using biotinylated USP25/28 inhibitor FT639 scheme (left panel); FT639 structure (based on FT224 inhibitor) and USP25/28 pulldown optimisation (right panel).

b FT639 enriched interactomes. FT639 interactome (left panel) and when competed with excess FT224. FT639 interactome at different concentrations using Dynabeads (left panel) or ultralink beads (middle and right panel) for enrichment by immunoprecipitation and quantitative mass spectrometry. Volcano plots are shown FT639 vs no probe control.

c RPS27A co-precipitates with FT639.

d RPS27L co-precipitates with FT639.

e Inhibition of translation elongation by interfering with deacetylated tRNA / blocking release of nascent polypeptide chain in the exit site of the ribosome. Illustration created using *www.bioart.niaid.nih.gov*.

Figure 4: USP28 Inhibitor off-target effects on protein translation

a Nascent protein synthesis in HAP1 cells affected by 4hrs exposure to USP28 inhibitor FT811 using the SunSet assay.

b Short-lived proteins affected by treatment of HAP1 cells with FT224 for 1 hr.

c FT224 compound exposure for 4 hrs affects protein synthesis in the OPP assay in HAP1 cells. Quantitation of data shown in panel **d**.

d Thienopyridine carboxamide inhibitors FT224, FT206 and FT811 affect nascent protein synthesis in HAP1 cells as measured by the OPP assay and assessed by microscopy.

e IC_{50} values of FT224, FT206 and FT811 in the OPP assay measured in HAP1 cells.

f Proteins in translation and ribosomal stalling in HAP1 cells affected by FT224, FT206 and FT811 in a dose and time-dependent manner.

Figure 5: USP28-FT592 complex structure and molecular basis for selective inhibition

a Structure of human USP28 in complex with FT592. FT592 is shown as a stick representation with carbon atoms colored green. The thumb, palm and fingers subdomains of the catalytic domain and catalytic cysteine, C171, are highlighted

b Left: view in panel **a** rotated on the y-axis by 50°; right: close-up view of the FT592 binding site highlighting secondary structural elements forming the binding pocket, key residues, and hydrogen-bonding interactions represented as dotted lines

c Superposition of human USP28 in complex with Ub-PA (USP28 colored violet, Ub-PA colored orange; PDB code 6HEI) on the USP28-FT592 complex structure colored grey. FT592 is shown as a stick representation with carbon atoms colored green. The catalytic cysteine, C171, is highlighted.

d Left: view in panel **c** rotated on the y-axis by 50°; right: close-up view of the FT592 binding site. The C-terminal tail of Ub-PA is shown in orange. The imidazole moiety of FT592 sterically clashes with the position of L73 in the C-terminal tail of Ub-PA, thereby preventing Ub binding and isopeptide bond cleavage.

e Left: superposition of human USP25 colored blue and the autoinhibitory motif (AIM) in the tetramer colored magenta (PDB code 6HEL) on the structure of the human USP28-FT592

complex colored grey with FT592 shown as a stick representation and carbon atoms colored green; right: close-up view of the FT592 binding site. Residues in AIM including the Pro-Phe motif (P521-F522) are shown as stick representations and labelled. FT592 sterically clashes with AIM in the autoinhibited USP25 tetramer.

f Left: superposition of apo form human USP7 colored gold (PDB code 1NB8) on the structure of the USP28-FT592 complex colored grey with FT592 shown as a stick representation and carbon atoms colored green; right: close-up view of the FT592 binding site highlighting the conformation of α5 in USP28 compared with α5 in USP7, which is kinked and reduces the volume of the pocket in USP7.

g Left: superposition of human apo form USP8 colored dark green (PDB code: 2GFO) on the structure of human USP28 in complex with FT206 colored grey with FT592 shown as a stick representation with carbon atoms colored green; right: close-up view of the FT592 binding pocket highlighting the conformation of α5 in USP28 compared with USP8 in which the helix is pivoted inwards reducing the volume of the pocket.

Figure items were prepared using PyMOL (The PyMOL Molecular Graphics System, Version 2.5.8, Schrödinger, LLC.).

Figure 6: USP25/28 inhibitors with and without off-target interference with protein synthesis

a OPP assay showing dose-dependent effects on protein synthesis for a panel of USP28 inhibitor compounds added to MCF7 cells. N=3 experiments.

b OPP assay showing effects on protein synthesis for a panel of USP28 inhibitors at 4 μM. N=3 experiments.

c OPP assay compound IC_{50} values (based on panel **a**).

d Correlation of compound OPP activity and effect on cell viability in MCF7 cells.

Figure 7: H-520 lung cancer cell susceptibility to USP28 inhibition due to on-target effect

a Wildtype MCF7 breast cancer cell confluence exposed to refined inhibitors for the indicated times at different concentrations. Two independent experiments with different panels of inhibitors are shown (N=8 each).

b USP28 KO MCF7 breast cancer cell confluence exposed to refined inhibitors for the indicated times at different concentrations. Two independent experiments with different panels of inhibitors are shown (N=8 each).

c H-520 squamous lung cancer cell confluence exposed to refined inhibitors for the indicated times at different concentrations. Left panel: 72 hrs; right panel: 24 hrs (N=8 each).

Table 1: Data collection and refinement statistics

Table 2: Antibodies used in this study

Figure 1

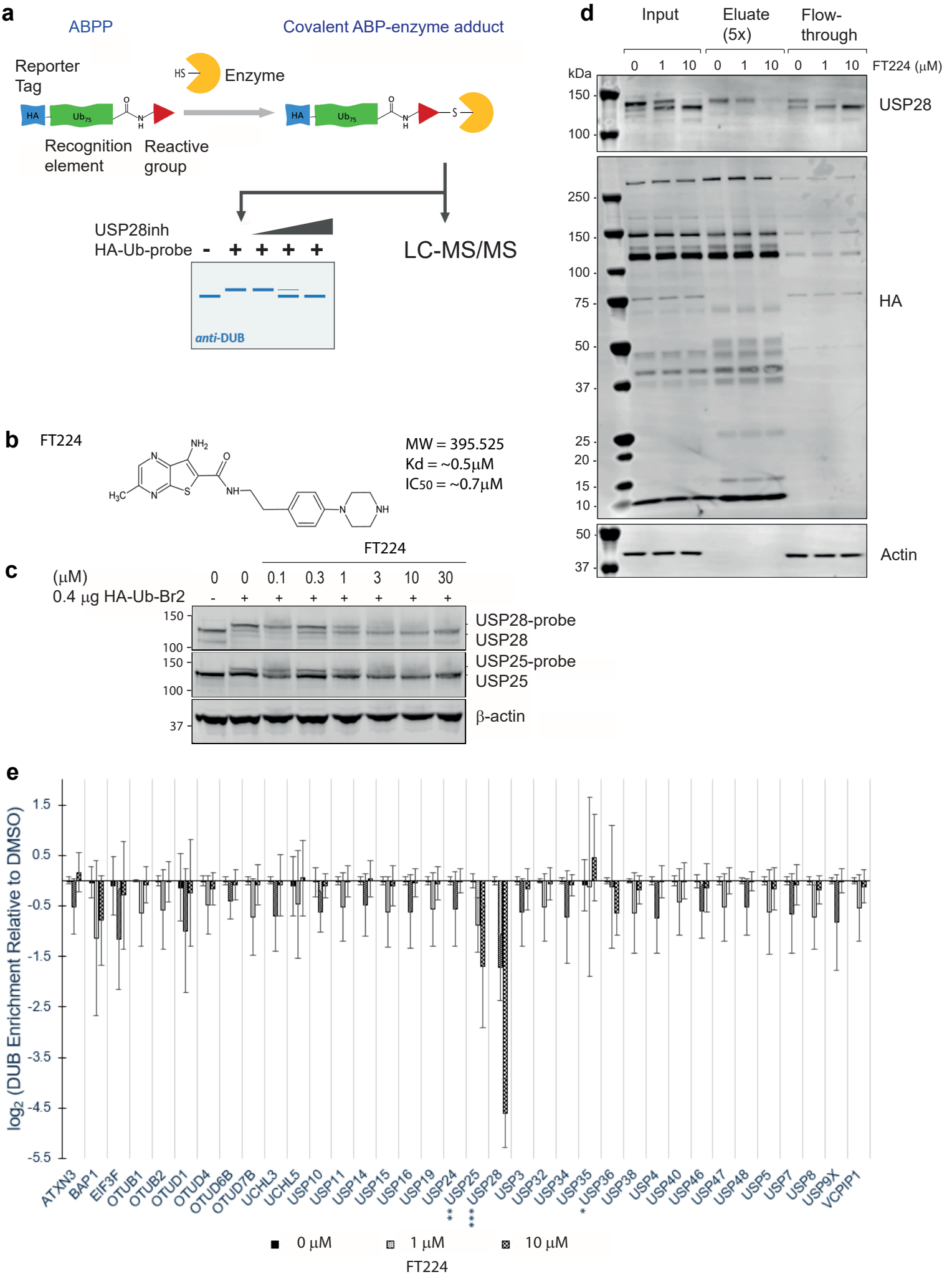
a
ABPP
Covalent ABP-enzyme adduct
Reporter Tag
Enzyme
HA
Ub75
Recognition element
Reactive group
USP28inh
HA-Ub-probe
- + + + +
LC-MS/MS
anti-DUB
b
FT224
MW = 395.525
Kd = ~0.5µM
IC50 = ~0.7µM
c
FT224
(µM)
0 0 0.1 0.3 1 3 10 30
0.4 µg HA-Ub-Br2
- + + + + + + +
USP28-probe
USP28
USP25-probe
USP25
β-actin
d
Input
Eluate (5x)
Flow-through
0 1 10 0 1 10 0 1 10 FT224 (µM)
kDa
USP28
HA
Actin
e
log2 (DUB Enrichment Relative to DMSO)
ATXN3 BAP1 EIF3F OTUB1 OTUB2 OTUD1 OTUD4 OTUD6B OTUD7B UCHL3 UCHL5 USP10 USP11 USP14 USP15 USP16 USP19 USP24 USP25 USP28 USP3 USP32 USP34 USP35 USP36 USP38 USP4 USP40 USP46 USP47 USP48 USP5 USP7 USP8 USP9X VCPIP1
0 µM
1 µM
10 µM
FT224

Figure 2

a

Proteome	HCT116 FBW7-/-	HCT116 FBW7+/+	FBW7+/+/ FBW7-/-
	FT224/ DMSO	FT224/ DMSO	DMSO/ DMSO
Cyclin D1 (CCND1)	-1.69	-1.49	-0.18
Cyclin B1 (CCNB1)	-0.91	-0.93	-0.31
Aurora A (AURKA)	-0.48	-0.44	-0.68
c-MYC	-0.76	-1.67	0.35
cJun	0.76	0.98	-0.58

b

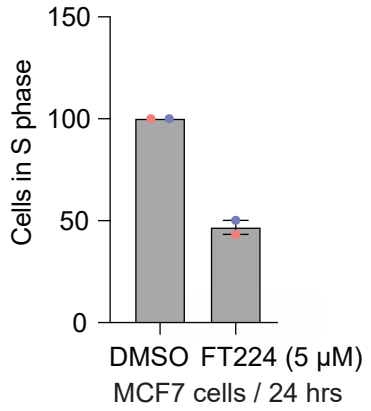

c

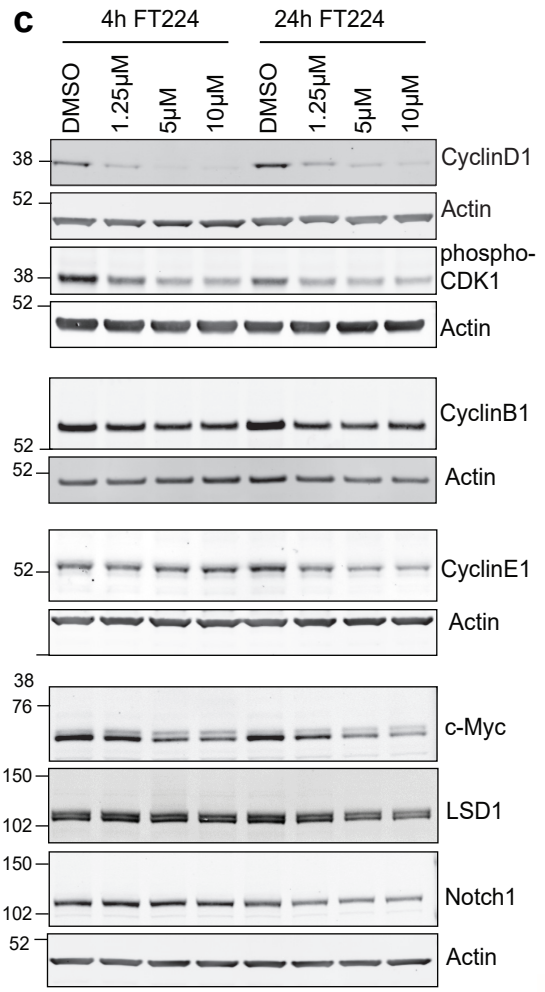

d

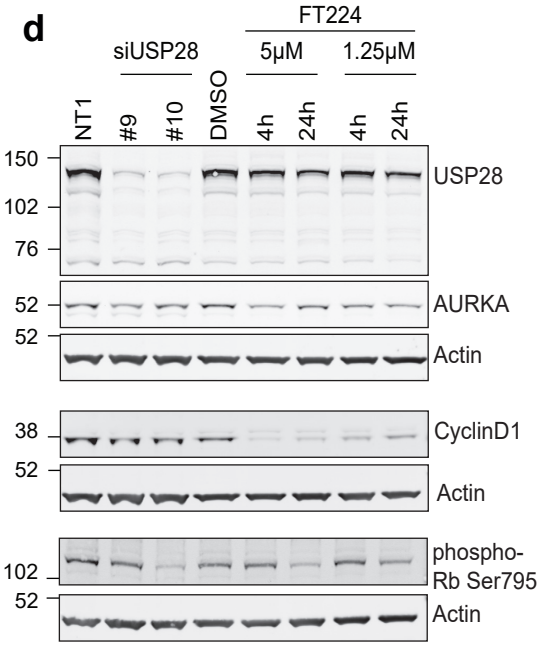

e

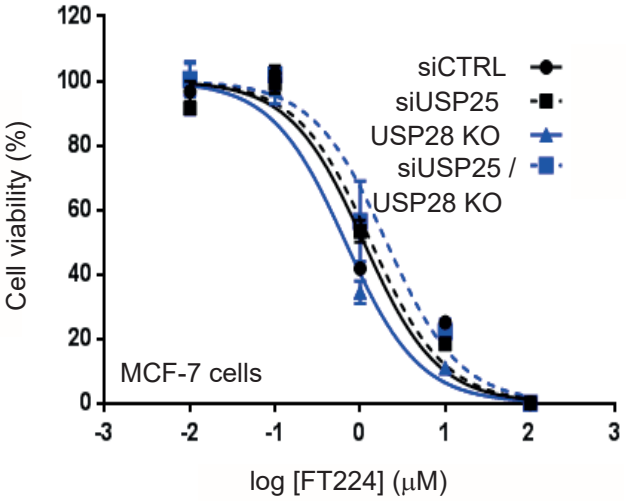

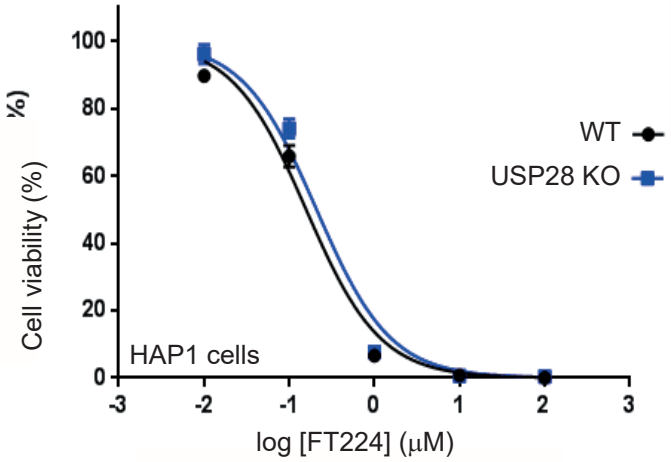

f

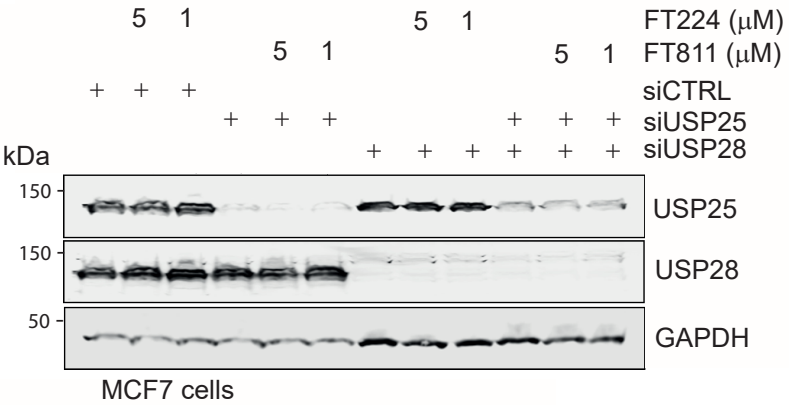

g

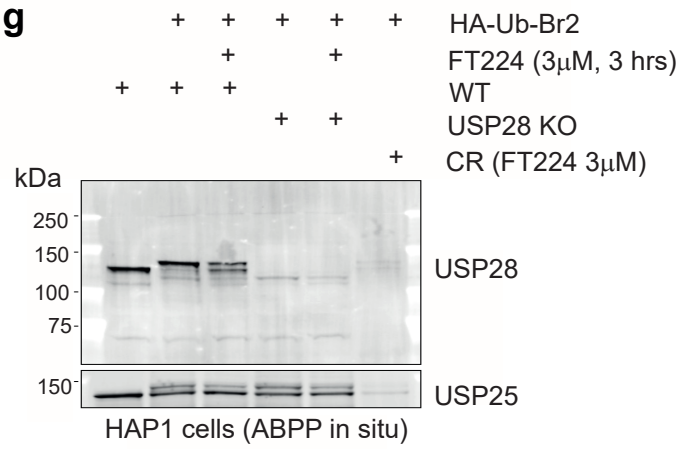

Figure 3

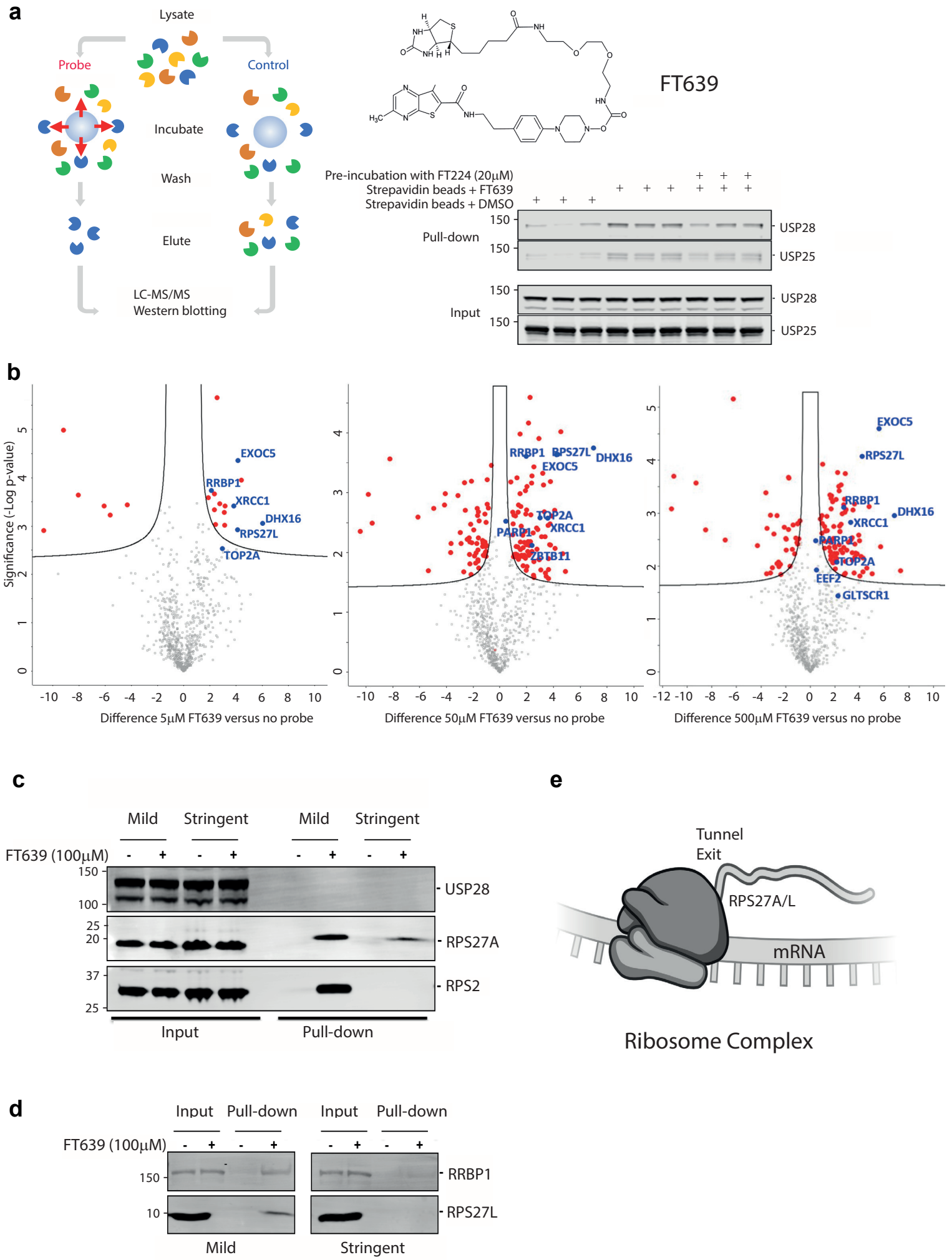
a
Lysate
Probe
Control
Incubate
Wash
Elute
LC-MS/MS
Western blotting
FT639
Pre-incubation with FT224 (20μM)
Strepavidin beads + FT639
Strepavidin beads + DMSO
Pull-down
Input
USP28
USP25
b
Significance (-Log p-value)
EXOC5
RRBP1
XRCC1
DHX16
RPS27L
TOP2A
PARP1
ZBTB11
EEF2
GLTSCR1
Difference 5μM FT639 versus no probe
Difference 50μM FT639 versus no probe
Difference 500μM FT639 versus no probe
c
Mild
Stringent
FT639 (100μM)
USP28
RPS27A
RPS2
Input
Pull-down
e
Tunnel
Exit
RPS27A/L
mRNA
Ribosome Complex
d
Input
Pull-down
FT639 (100μM)
RRBP1
RPS27L
Mild
Stringent

Figure 4

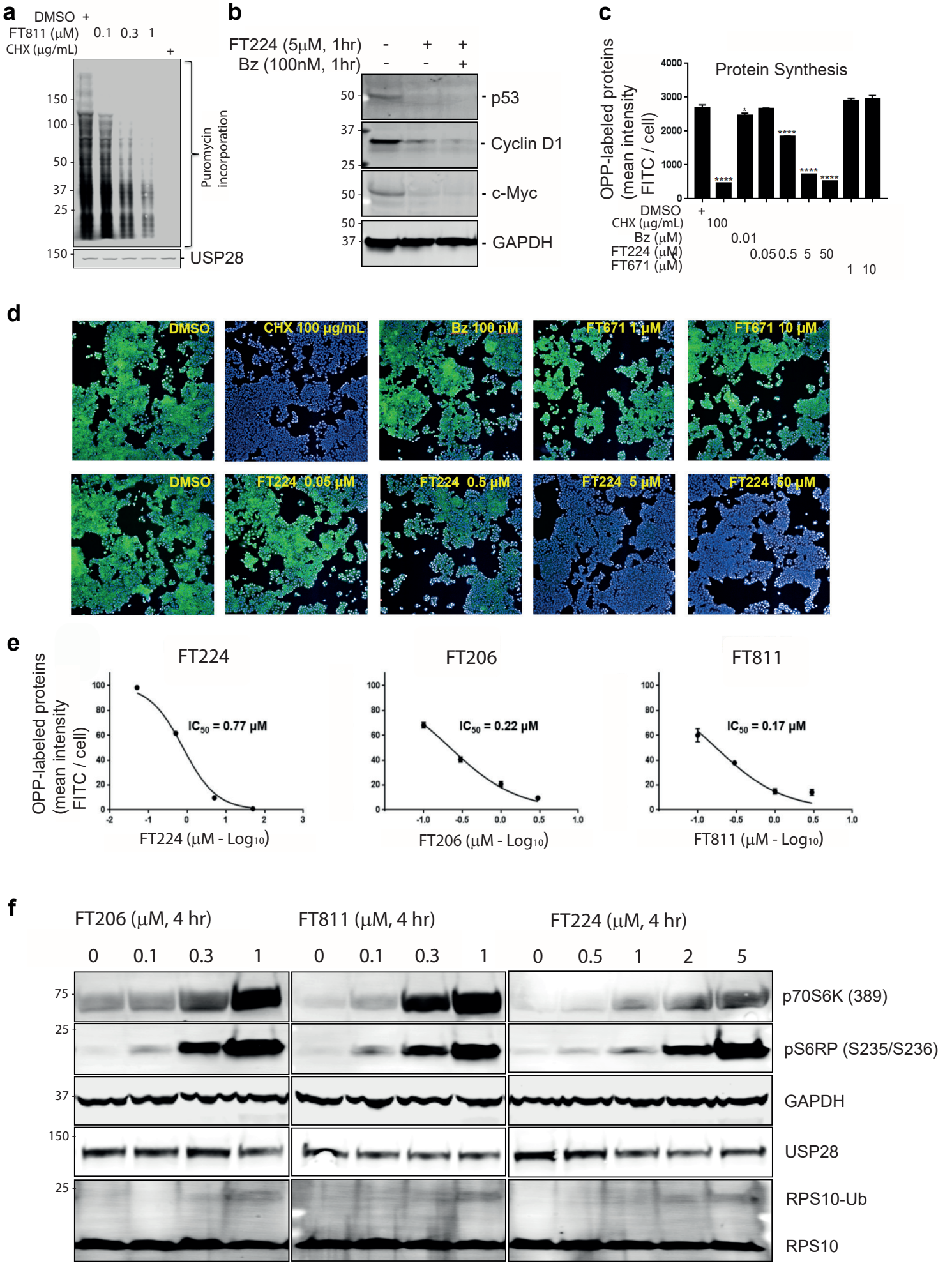
a
DMSO +
FT811 (μM) 0.1 0.3 1
CHX (μg/mL) +
150
100
50
37
25
Puromycin incorporation
150
USP28
b
FT224 (5μM, 1hr) - + +
Bz (100nM, 1hr) - - +
50
p53
37
Cyclin D1
25
50
c-Myc
50
37
GAPDH
c
Protein Synthesis
OPP-labeled proteins (mean intensity FITC / cell)
4000
3000
2000
1000
0
DMSO +
CHX (μg/mL) 100
Bz (μM) 0.01
FT224 (μM) 0.05 0.5 5 50
FT671 (μM) 1 10
d
DMSO
CHX 100 μg/mL
Bz 100 nM
FT671 1 μM
FT671 10 μM
DMSO
FT224 0.05 μM
FT224 0.5 μM
FT224 5 μM
FT224 50 μM
e
OPP-labeled proteins (mean intensity FITC / cell)
FT224
IC50 = 0.77 μM
FT224 (μM - Log10)
FT206
IC50 = 0.22 μM
FT206 (μM - Log10)
FT811
IC50 = 0.17 μM
FT811 (μM - Log10)
f
FT206 (μM, 4 hr)
0 0.1 0.3 1
FT811 (μM, 4 hr)
0 0.1 0.3 1
FT224 (μM, 4 hr)
0 0.5 1 2 5
75
p70S6K (389)
25
pS6RP (S235/S236)
37
GAPDH
150
USP28
25
RPS10-Ub
RPS10

Figure 5

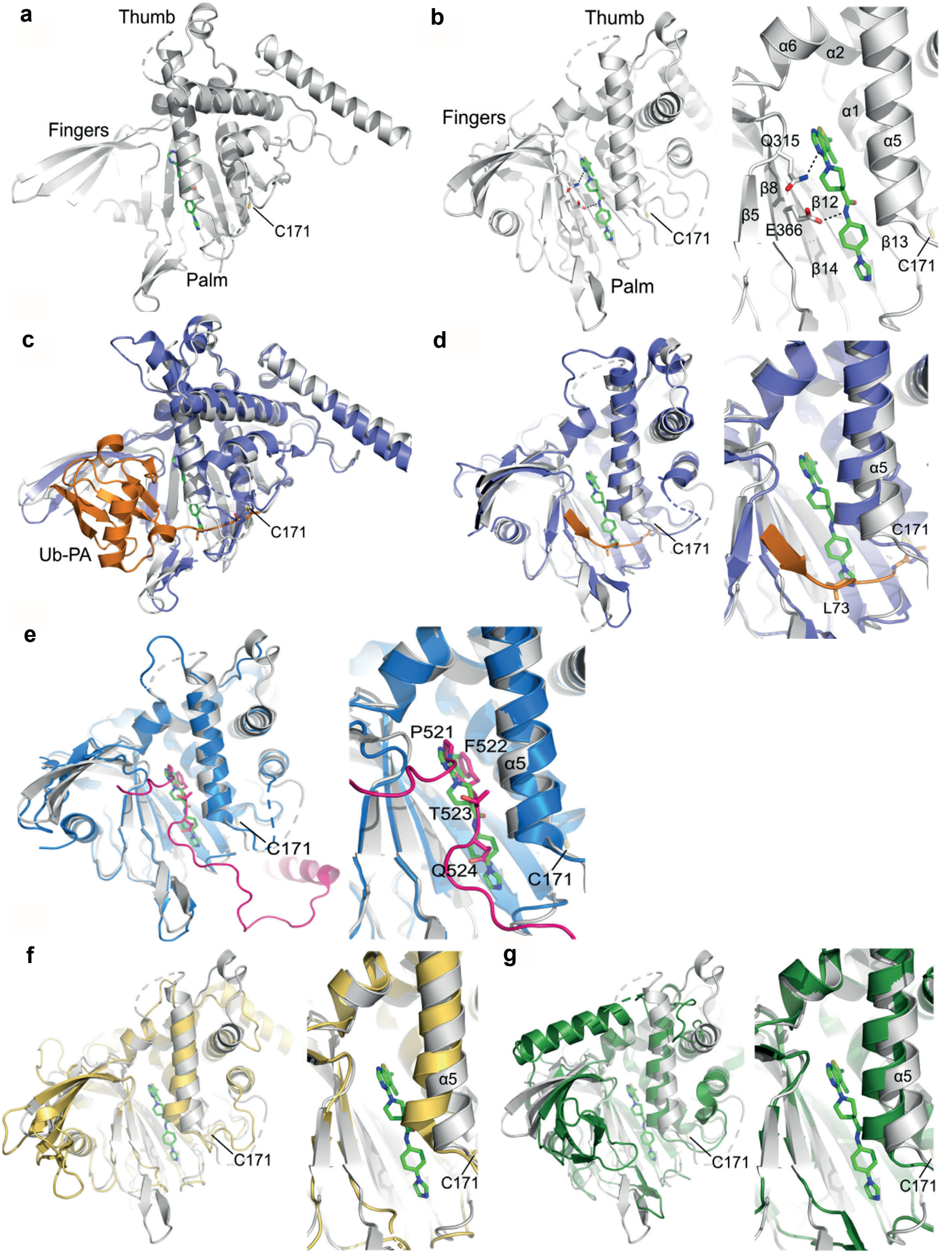
a
Thumb
Fingers
C171
Palm
b
Thumb
Fingers
C171
Palm
α6
α2
α1
α5
Q315
β8
β12
β5
E366
β13
β14
C171
c
C171
Ub-PA
d
C171
α5
C171
L73
e
C171
P521
F522
α5
T523
Q524
C171
f
C171
α5
C171
g
C171
α5
C171

Figure 6

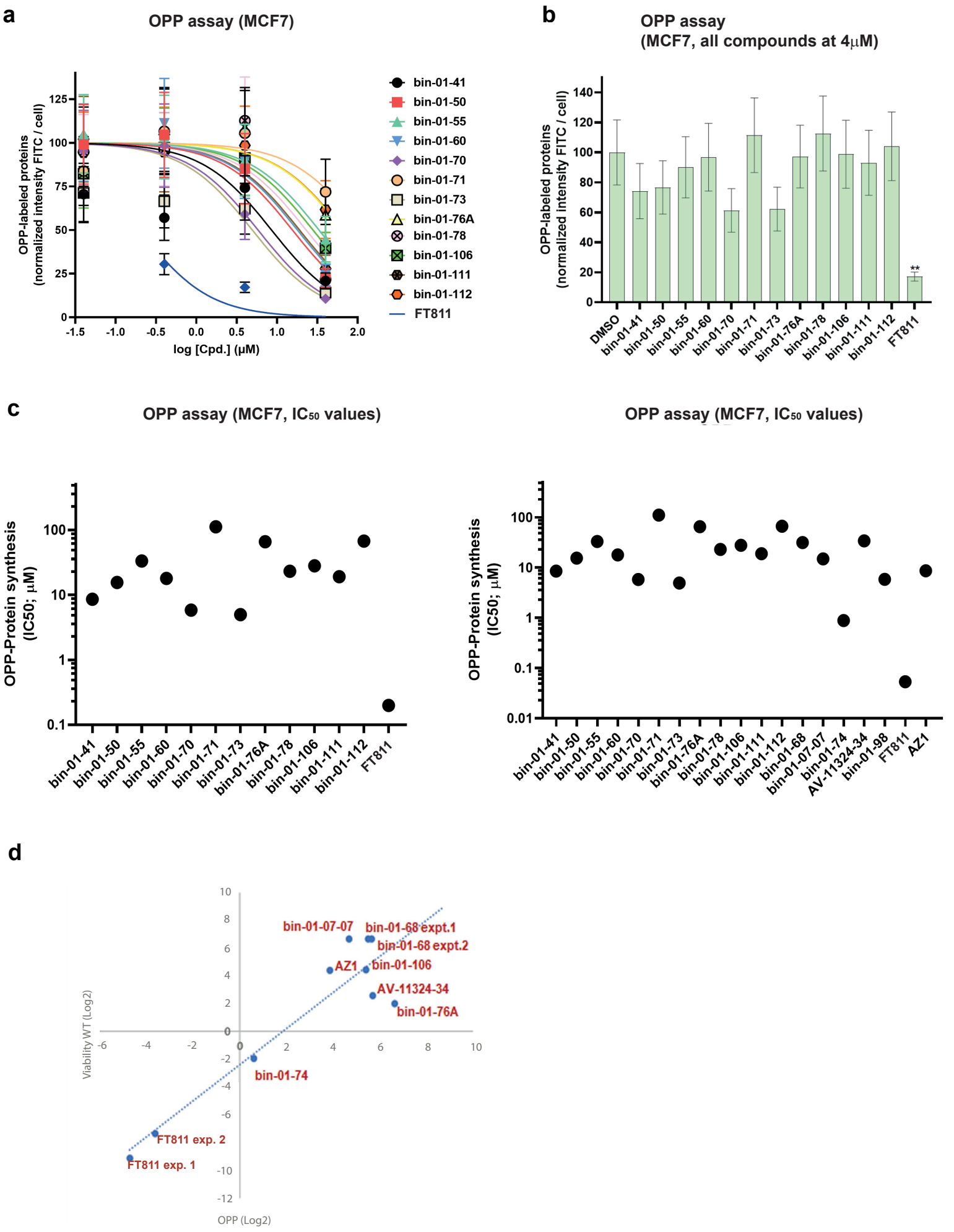
a
OPP assay (MCF7)
OPP-labeled proteins (normalized intensity FITC / cell)
log [Cpd.] (μM)
bin-01-41
bin-01-50
bin-01-55
bin-01-60
bin-01-70
bin-01-71
bin-01-73
bin-01-76A
bin-01-78
bin-01-106
bin-01-111
bin-01-112
FT811
b
OPP assay
(MCF7, all compounds at 4μM)
OPP-labeled proteins (normalized intensity FITC / cell)
DMSO
bin-01-41
bin-01-50
bin-01-55
bin-01-60
bin-01-70
bin-01-71
bin-01-73
bin-01-76A
bin-01-78
bin-01-106
bin-01-111
bin-01-112
FT811
c
OPP assay (MCF7, IC50 values)
OPP-Protein synthesis (IC50; μM)
OPP assay (MCF7, IC50 values)
OPP-Protein synthesis (IC50; μM)
bin-01-41
bin-01-50
bin-01-55
bin-01-60
bin-01-70
bin-01-71
bin-01-73
bin-01-76A
bin-01-78
bin-01-106
bin-01-111
bin-01-112
bin-01-68
bin-01-07-07
bin-01-74
AV-11324-34
bin-01-98
FT811
AZ1
d
Viability WT (Log2)
OPP (Log2)
bin-01-07-07
bin-01-68 expt.1
bin-01-68 expt.2
AZ1
bin-01-106
AV-11324-34
bin-01-76A
bin-01-74
FT811 exp. 2
FT811 exp. 1

Figure 7

a

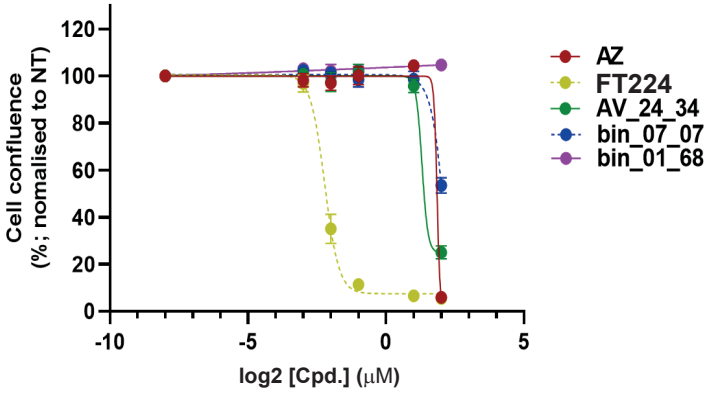
USP28i (MCF7, Incucyte, 72 hrs) - exp. 1
Cell confluence (%; nomalised to NT)
log2 [Cpd.] (μM)
AZ
FT224
AV_24_34
bin_07_07
bin_01_68

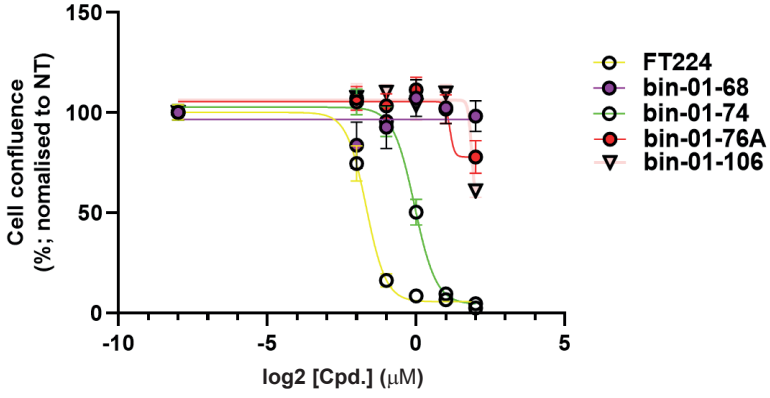
USP28i (MCF7, Incucyte, 72 hrs) - exp. 2
Cell confluence (%; nomalised to NT)
log2 [Cpd.] (μM)
FT224
bin-01-68
bin-01-74
bin-01-76A
bin-01-106

b

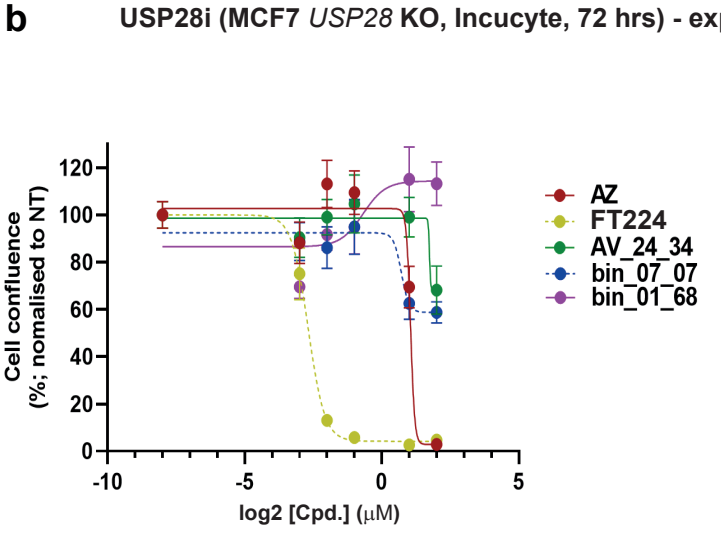
USP28i (MCF7 USP28 KO, Incucyte, 72 hrs) - exp. 1
Cell confluence (%; nomalised to NT)
log2 [Cpd.] (μM)
AZ
FT224
AV_24_34
bin_07_07
bin_01_68

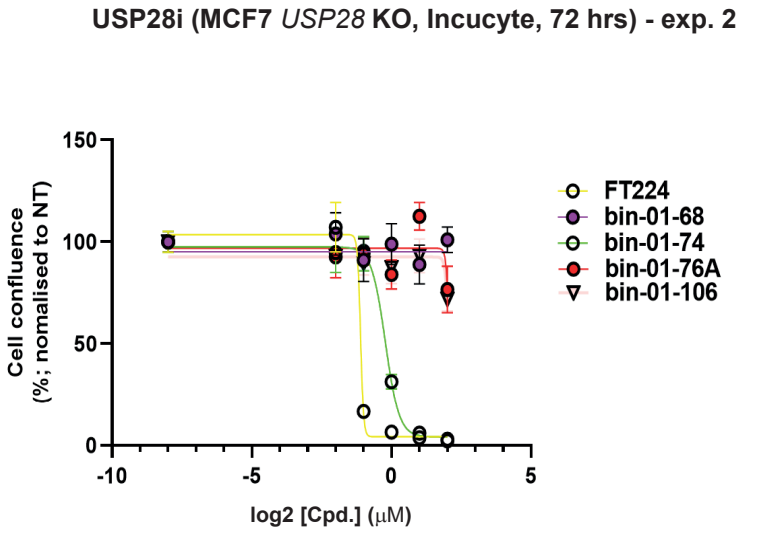
USP28i (MCF7 USP28 KO, Incucyte, 72 hrs) - exp. 2
Cell confluence (%; nomalised to NT)
log2 [Cpd.] (μM)
FT224
bin-01-68
bin-01-74
bin-01-76A
bin-01-106

c

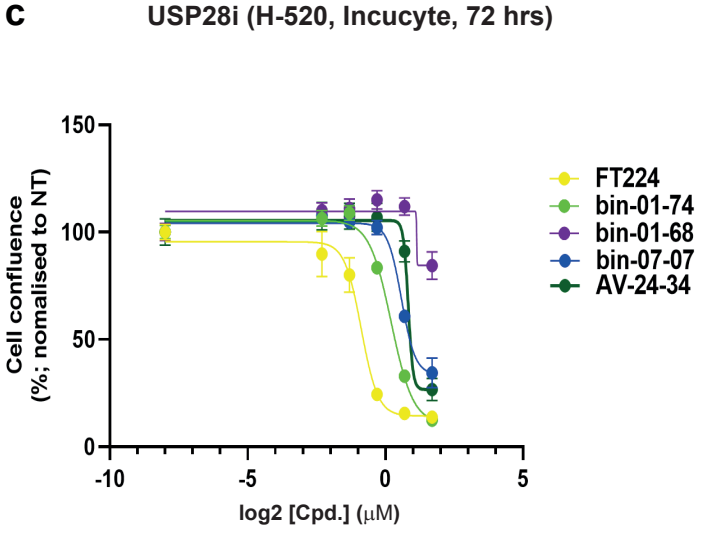
USP28i (H-520, Incucyte, 72 hrs)
Cell confluence (%; nomalised to NT)
log2 [Cpd.] (μM)
FT224
bin-01-74
bin-01-68
bin-07-07
AV-24-34

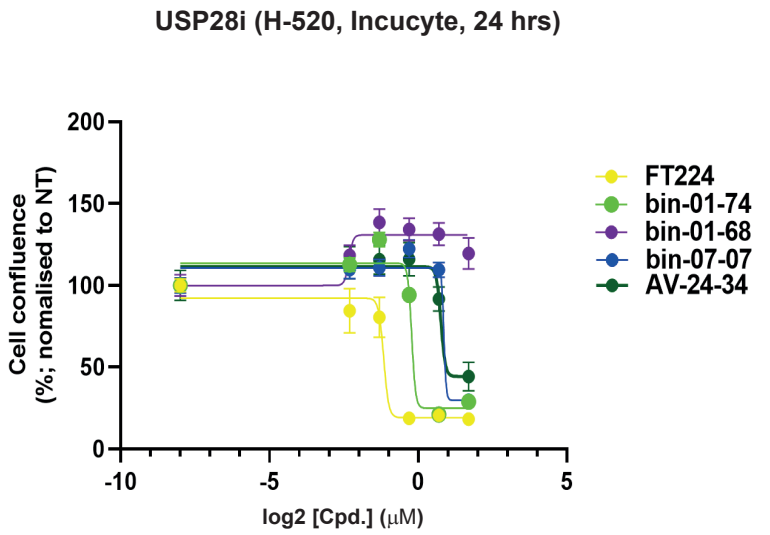
USP28i (H-520, Incucyte, 24 hrs)
Cell confluence (%; nomalised to NT)
log2 [Cpd.] (μM)
FT224
bin-01-74
bin-01-68
bin-07-07
AV-24-34

Table 1: Data collection and refinement statistics

USP28-FT592 complex	
Data collection	
Space group	H32
Cell dimensions	
a, *b*, *c* (Å)	107.8, 107.8, 274.7
Resolution (Å)	29.45 - 3.40 (3.52 - 3.40)
R_{merge}	0.139 (0.476)
$< I / \sigma I >$	8.9 (2.1)
Completeness (%)	99.9 (100.0)
Redundancy	6.10 (4.62)
Refinement	
Resolution (Å)	29.00-3.40
No. reflections (test set)	8356 (393)
R_{work} / R_{free}	0.229 (0.280)
No. atoms	
Protein	2584
Ligand	31
B-factors (Å^2)	
Protein	101.0
Ligand	110.0
R.m.s. deviations	
Bond lengths (Å)	0.0106
Bond angles (°)	1.8484
Ramachandran (%) Preferred/Allowed/Outliers	90.0/9.4/0.6

Values in parentheses are for the highest resolution shell. Data set collected and structure determined from a single crystal.

Table 2: Antibodies used in this study

Antibody name	Group	Raised in	Source	Catalog numbe	Concentration/time
Actin	Cytoskeleton	Rabbit	Sigma	A2266	1:2000 1hr. 1:10000 2.5 % BSA
Actin	Cytoskeleton	Mouse	Abcam	Ab6276	1:10,000, 50 mins
Beta-actin	Cytoskeleton	Mouse	Cell Signaling	3700	1:1000 o/n
CDK1NA (p21)	Cell cycle	mouse	Santa Cruz	sc-6246	1:200, O/N
c-Jun	Transcription Factor	Mouse	BD Transduction labor	610326	1:1000 o/n
c-Myc	Transcription Factor	Rabbit	Cell Signaling	#5606	1: 1000 O/N
c-Myc	Transcription Factor	Rabbit	Cell Signaling	13987	1:1000 o/n
Cyclin B1	Cell cycle	Mouse	Abcam	05-373	1:1000, 1hr or o/n
Cyclin D1	Cell cycle	mouse	Santa Cruz	sc-8396	1:1000, O/N
Cyclin D1	Cell cycle	Rabbit	Cell Signaling	2922	1:1000 o/n
Cyclin E1	Cell cycle	Mouse	Cell Signalling	HE12	1:1000, o/n
EEF2	Translatoin	Rabbit	Cell Signaling	2332	1:1000 o/n
Fbw7	E3-Ligase etc	Rabbit	Bethyl	A301-720A	1:1000, O/N
GAPDH	Metabolism	Mouse	Invitrogen	MA5-15738	1:1000 o/n
GST Tag Monoclonal Antibody (8-326)	GST-tag	Mouse	Invitrogen	MA4-004	1:1000 o/n
HA	Hemagluttinin tag	Mouse	Roche	11666606001	1:2000 o/n
LSD1	Chromatin	Mouse mAb	Cell Signaling	#4218	1:1000 o/n or 1hr
Notch1	Transcription	Rabbit mAb	Cell Signaling	#3608	1:1000
p21/Waf1/Cip	Signalling	Rabbit	Cell Signaling	2947	1:1000 o/n
p4EBP1 (Thr 37/46)	Translatoin	Rabbit	Cell Signaling	2855	1:1000 o/n
p53	Transcription Factor	Mouse	Cell Signaling	2524	1:1000 o/n
p70S6K (Thr389)	Signalling	Rabbit	Cell Signaling	9234	1:1000 o/n
pAKT (Ser 473)	Signalling	Rabbit	Cell Signaling	4060	1:1000 o/n
pCDK1	Cell cycle	Rabbit	Cell Signalling	9111	1:1000, o/n
pEEF2 (Tyr 56)	Translation	Rabbit	Cell Signaling	2331	1:1000 o/n
PRAME	Translation	Rabbit	Cell Signaling	45084	1:1000 o/n
PS6RP (Ser 235/236)	Signalling	Rabbit	Cell Signaling	4858	1:1000 o/n
Puromycin	Translation	Mouse	Merck - Millipore	MABE343	1:1000 o/n
RPS10	Ribosome	Rabbit	Abcam	Ab151550	1:1000 o/n
RPS2	Ribosome	Rabbit	Abcam	ab155961	1:1000 o/n
RPS27A	Ribosome	Rabbit	Invitrogen	PA5-141043	1:1000 o/n
RPS27L	Ribosome	Rabbit	Abcam	Ab221904	1:1000 o/n
RRBP1	Ribosome	Mouse	Invitrogen	MA5-18289	1:1000 o/n
Streptavidin (IRDYE 800CW)	Biotin-specific	N/A	Licor Biosciences	926-32230	1:1000 o/n
Ubiquitin	Protein turnover	Mouse	Merck - Millipore	MAB5486	1:1000 o/n
USP25	DUB	Rabbit	Abcam	ab187156	1:1000 o/n
USP28	DUB	Rabbit	Abcam	ab126604	1:1000 1h or o/n
USP28	DUB	Goat	Abcam	ab130351	1:1000 1hr RT
680RD Goat anti-Mouse IgG Secondary Antibody	Secondary Antibody	Goad	Licor Biosciences	926-68070	1:20,000
800RD Goat anti-Rabbit IgG Secondary Antibody	Secondary Antibody	Goad	Licor Biosciences	926-32211	1:20,000